

Gross Structure in  $(d,p)$  Reactions near  $Z=50$ R. A. PECK, JR., *Brown University, Providence, Rhode Island*

AND

J. LOWE, *University of Birmingham, Birmingham, England*

(Received June 18, 1958; revised manuscript received January 12, 1959)

Proton spectra from  $\text{Sn}^{120}(d,p)\text{Sn}^{121}$  and  $\text{In}^{115}(d,p)\text{In}^{116}$  at 19.7 Mev are presented, covering 6.5 Mev of excitation in the product nucleus and laboratory angles from  $15^\circ$  to  $155^\circ$  at  $10^\circ$  intervals. The reactions are closely similar in all characteristics. Broad energy groups are discussed relative to the correlation with neutron single-particle states anticipated by a giant-resonance interpretation of their nature. Of four such groups identified, the spectral locations of three agree quantitatively with the single-particle level scheme deduced from binding-energy data. A group at 0.8 Mev, while consistent with single-particle gross structure, may represent a distinct nuclear level enhanced for reasons not clear. Angular distributions for the several groups fail to show the strong minima characteristic of pure stripping forms, probably as a consequence of the spreading of single-particle levels resulting from finite nuclear distortion which also weakens the spectral gross structure. However, the slight structure which the distributions do display is qualitatively consistent with stripping peak positions consequent on the single-particle interpretation of the spectra.

## INTRODUCTION

MANY types of nuclear reactions, for nuclei whose levels are closely spaced relative to the experimental resolution interval, exhibit in their spectra a gross structure<sup>1</sup> of energy groups with widths and spacings of Mev order. Similar "giant resonances" in neutron cross sections are related in formal reaction theory to broad maxima appearing in the average neutron strength function when coupling between nucleon and core is intermediate<sup>2</sup> in strength, i.e., not sufficiently strong to dispel altogether the single-particle level organization of the extreme shell model. The possibility of a similar account of the gross structure in other reaction types<sup>3</sup> may be investigated by comparison of gross structure positions and angular distributions with the appropriate single-particle level locations and orbitals. For such a study the  $(d,p)$  reaction is doubly satisfactory, offering a reliable formalism for angular distribution analysis (stripping theory) and involving, in the first 7 Mev of excitation, a unique set of single-particle levels (bound neutrons). It is quite possible, furthermore, that single-particle levels may be preferentially excited by the  $(d,p)$  reaction and collective ones by inelastic scattering.<sup>4</sup>

The target nuclei chosen for this experiment,  $^{49}\text{In}^{115}$  and  $^{50}\text{Sn}^{120}$ , are sufficiently heavy to satisfy the resolution condition defining the gross structure problem. In

neutron complement they are similar, representing even- $N$  cores within a shell, but they are proton-magic and nonmagic, respectively, and so differ somewhat in nuclear distortion. It follows that one may anticipate resemblances between the two reactions in such features as are principally determined by the population of single-neutron levels in an undistorted well, and differences in any characteristics depending strongly upon nuclear shape.

## EXPERIMENTAL

Metallic foils ( $\text{In}^{115}$ , 96%, 9.16 mg/cm<sup>2</sup> and  $\text{Sn}^{120}$ , 98%, 18.15 mg/cm<sup>2</sup>) were bombarded by deuterons of energy  $19.7 \pm 0.15$  Mev from the Nuffield cyclotron of the University of Birmingham and resulting protons studied in a scattering chamber and with detectors and instrumentation developed by Greenlees and co-workers.<sup>5</sup> The counter angle relative to the deuteron beam has a fixed elevation ( $15^\circ$ ) above the horizontal plane, its horizontal projection being adjustable to any value to well within  $1^\circ$ . The target angle was set approximately at the value for maximum resolution at each angle (minimum combined energy loss of deuteron and proton in the target).

A circular aperture defines the solid angle ( $3.70 \times 10^{-4}$  steradian) of the detector, which consists of a thin (1 mm) and a thick (3 mm) CsI(Tl) crystal in series in the proton path. Pulse-height distributions from the thick crystal are displayed on a Hutchinson-Scarrott pulse-height analyzer (of 60 or 80 channels, alternatively) gated by the output of a single channel discriminator monitoring the thin-crystal pulse. The gating window width was generally about 20 volts, terminating about 10 volts from the deuteron peak and serving to exclude most of the elastically scattered

<sup>1</sup> B. L. Cohen *et al.*, Phys. Rev. **105**, 1549; **106**, 995 (1957); L. Colli and S. Micheletti, Nuovo cimento **6**, 1001 (1957); J. A. Harvey, Phys. Rev. **81**, 353 (1951); H. E. Gove, Phys. Rev. **81**, 365 (1951); D. L. Allan, Proc. Phys. Soc. (London) **A70**, 195 (1957); R. A. Peck, Jr., Phys. Rev. **106**, 965 (1957).

<sup>2</sup> Lane, Thomas, and Wigner, Phys. Rev. **98**, 693 (1955).

<sup>3</sup> The issue was first brought to the authors' attention by A. V. Cohen and elaborated verbally by A. M. Lane and G. E. Brown, in 1956. The first suggestion in print appears to be that of B. L. Cohen, reference 1, and the clearest statement by Schiffer, Lee, Yntema, and Zeidman, Phys. Rev. **110**, 1216 (1958). Early work on a single-particle interpretation of  $(d,p)$  spectra is that of M. H. L. Pryce, Proc. Phys. Soc. (London) **A65**, 773 (1952).

<sup>4</sup> We are indebted to Professor W. E. Burcham for this observation.

<sup>5</sup> Greenless, Haywood, Kuo, and Petravac, Proc. Phys. Soc. (London) **A70**, 331 (1957); Proc. Roy. Soc. (London) **A243**, 206 (1957).

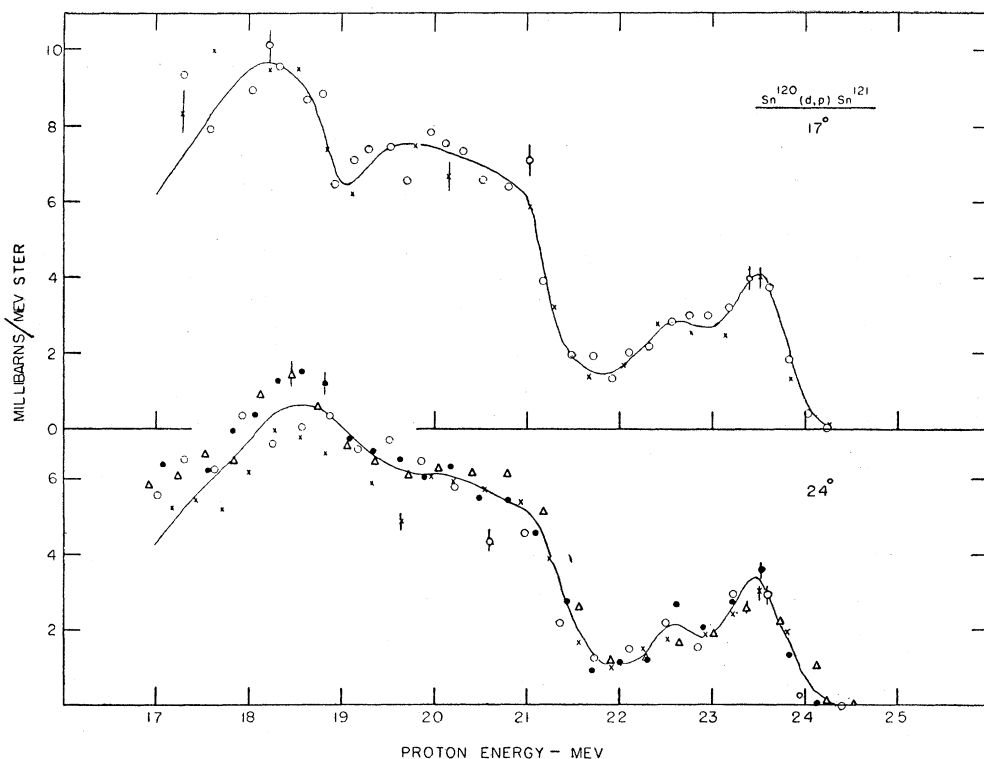


FIG. 1. Sample data at two laboratory angles. The two independent determinations (above) and four (below) were made with assorted target angles, amplifications, and channel sizes. Typical magnitudes of counting probable error ( $\pm 0.67N^{1/2}$ ) are shown for each data set. The solid curves are the visual best fits representing  $17^\circ$  and  $24^\circ$  in Fig. 2.

deuterons and gamma ray background without loss of high-energy protons. Low counting rates obviated the need for dead time corrections, and visual monitoring of the kicksorter throughout its operation is thought to have detected most instances of spurious recording. A variety of electronic parameters (analyzer bias, channel size, and amplification) were employed and the various laboratory angles investigated in irregular order and interspersed with background and calibration runs.

Auxiliary experiments provided direct calibrations of the following systematic quantities: numerical correspondence of analyzer bias, gain, and channel size; intensity loss through pulses falling between analyzer channels (3%); effective thickness of thin crystal for reaction protons; pulse-height—energy relation for thick crystal. The last was found linear for both protons and deuterons, with the same slope for the two within experimental uncertainty (2%) and slightly but significantly different intercepts (for zero pulse height,  $-0.3$  Mev for deuterons and  $+0.4$  Mev for protons). Crystal resolution was 6% for 9.8-Mev protons and 4% for 19.6-Mev deuterons. With these calibrations, the translation of pulse height to primary proton energy was absolute. The maximum energy

group at every angle fell within about 0.5 channel of that computed from the established  $Q$  values.<sup>6</sup>

Because the experiment turns on identification of significant structure in the spectra, observed intensities of easily identifiable groups (elastically scattered protons and deuterons in calibration runs and the clearly reproduced high-energy doublet in the reaction spectra) were scrutinized carefully for systematic effects. The analysis showed that the observed fluctuations are accurately represented by counting statistics and that each of the varied experimental conditions is free of systematic effect on observed intensity. For 70 intensity comparisons the mean ratio of observed deviation to counting probable error is 1.05, with 36 values above unity and 34 below. The distribution of observed variations falls accurately on the absolute normal curve of error, deviating at most by 20% of the counting error and generally by less than 5% of it. A systematic intensity effect is introduced by the non-linearity of the relation between channel number and primary proton energy which is a consequence of the large basic absorption introduced by the gating crystal. The effect has been removed by dividing the yield in each channel (millibarns/steradian channel) by the local channel width (Mev of primary proton energy/

<sup>6</sup> Indium,  $+4.16$  Mev; Sn,  $+3.92$  Mev; D. W. Van Patter and W. Whaling, *Revs. Modern Phys.* **26**, 402 (1954).

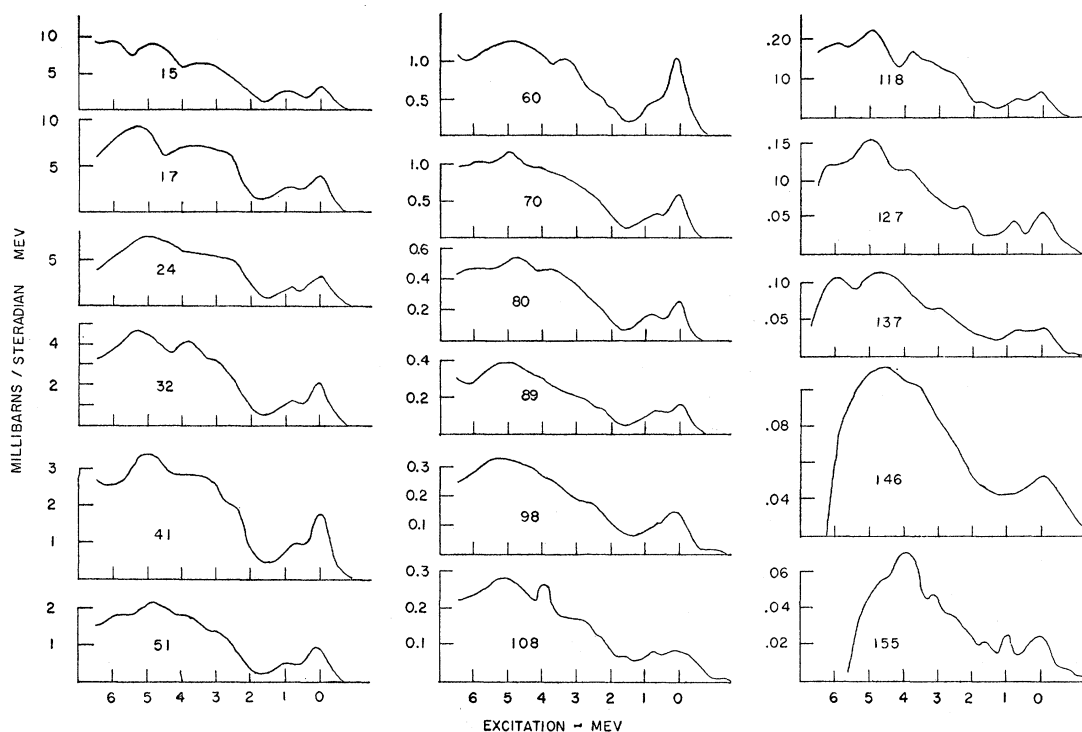


FIG. 2. Collected spectra for  $\text{Sn}^{120}(d, p)\text{Sn}^{121}$  at laboratory angles as labeled. Abscissa is residual nucleus excitation ( $Q_0 - Q$ ) for all curves, and curves are visual best fits to data from the following numbers of independent determinations: 5,  $41^\circ$ ; 4,  $24^\circ$ ,  $60^\circ$ ; 3,  $15^\circ$ ,  $32^\circ$ ,  $51^\circ$ ; 2,  $17^\circ$ ,  $70^\circ$ ,  $80^\circ$ ,  $98^\circ$ ,  $137^\circ$ ; 1 determination each at remaining angles. The dip at highest excitation is instrumental.

channel). This correction for channel nonuniformity amounts to 1.5:1.0 over the spectral range presented and results, in the final spectra, in a relatively increased cross section for lower proton energy. Uncertainty associated with the removal of residual background casts doubt on the highest 1 Mev of excitation presented for the largest two angles, but otherwise the spectra are free of systematic effect throughout the regions presented.

All spectra taken for a given laboratory angle were translated to absolute coordinates and superposed on a single graph, in which form they agreed well both on energy and cross section scales. Throughout the spectrum the various data sets fell within the counting probable error about half the time and usually within the combined probable errors, although the yield in individual channels was markedly less reproducible than was the integrated intensity of a clear group (preceding paragraph). On each composite graph a representative spectrum was drawn visually, incorporating only structure indicated at least qualitatively by every contributing data set. Sample data and representative curves are shown in Fig. 1.

### RESULTS

The representative spectra at all angles are displayed in Figs. 2 and 3. The dip at highest excitations is instrumental, produced by the action of the electronic

gate as shown by its location on the energy scale. Figures 4 and 5 show the total energy spectra for the two reactions, obtained by numerical integration of the representative curves over angle. The similarity of the two reactions is evident; an extra group appearing for In is a consequence of the greater excitation range accessible as a result of that reaction's larger  $Q$ .

The dashed groups, representing the slight gross structure which is reproducible in the spectra, are clearly not uniquely deducible from Figs. 4 and 5, above 2 Mev of excitation. The identification of any possible spectral structure is a necessary prerequisite to the display of meaningful angular distributions, however, in order to suggest relevant abscissas at which to sample those distributions. The identification of structure is justified by the recurrence at the various angles of deviations from monotonic spectra which are sustained over several successive channels, clearly exceed statistical fluctuations, and occur in roughly the same spectral areas. The positions of these recurrent deviations from uniformity, read for each angle in Figs. 2 and 3 and averaged, define the mean "peak" positions in Table I with the mean deviations there shown. The dashed groups in Figs. 4 and 5 were obtained by assuming symmetrical groups centered at these mean positions, the total spectra being decomposed by the usual method of successive reflection of exposed high-energy profile and subtraction. Thus the

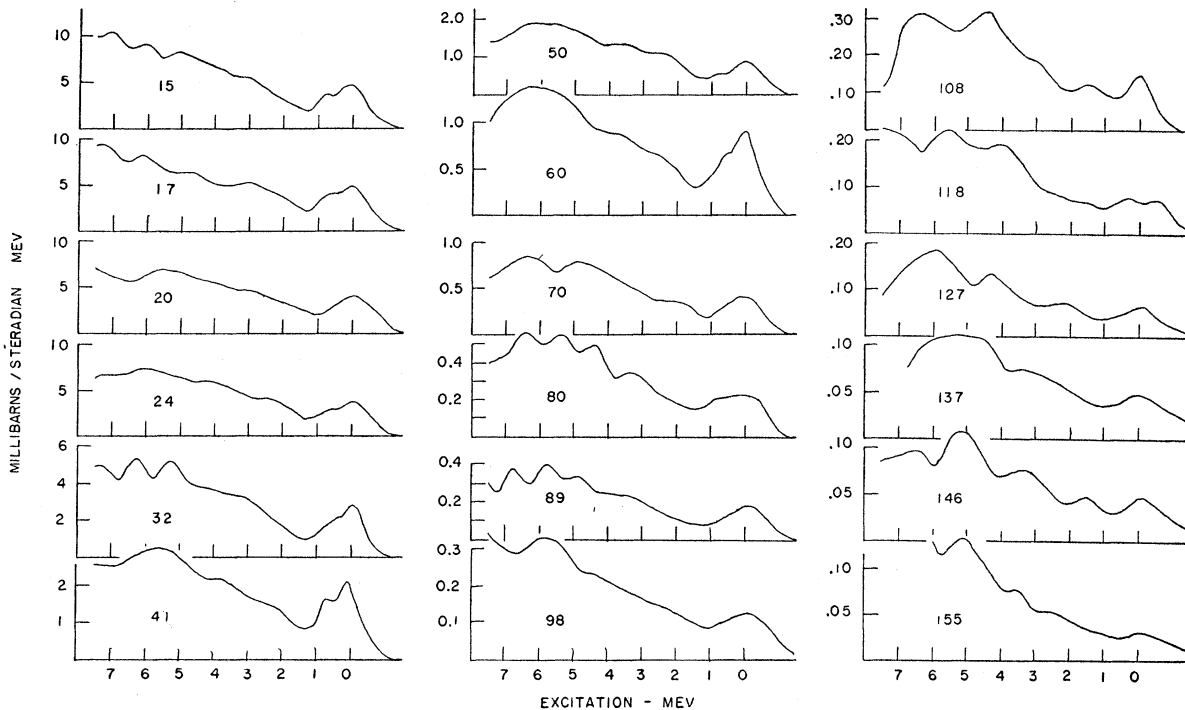


FIG. 3. Collected spectra for  $\text{In}^{115}(d,p)\text{In}^{116}$  at laboratory angles as labeled. Numbers of independent determinations: 5, 41°; 3, 24°, 50°; 2, 15°, 17°, 60°, 70°, 98°; 1 determination each at remaining angles.

dashed representation of gross structure in these spectra, summarized in Table I, has the following significance: group positions represent within the mean deviations shown the loci of recurrent, sustained deviations from uniform spectra and the number of groups is the minimal number of such regular deviations. Only the widths, and hence also the separate group cross sections, are dependent upon a decomposition of Figs. 4 and 5.

The angular distributions (Figs. 6 and 7) are of

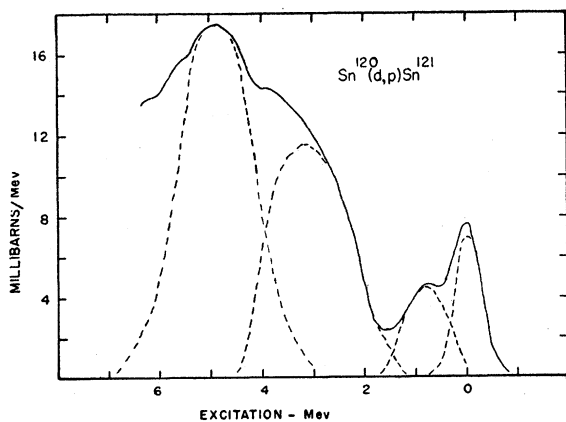


FIG. 4. Energy spectrum for  $\text{Sn}^{120}(d,p)\text{Sn}^{121}$  obtained by integration over laboratory angles of Fig. 2. Dotted curves represent minimal gross structure groups, their positions determined by averaging occurrences at various angles. These groups are summarized in Table I.

ordinates at fixed excitation rather than total group contents integrated over energy. This method of display is justified by the fact that well defined groups, e.g., of elastically scattered particles, are seen not to vary appreciably in width with variation in angle. The various groups are sampled at excitations appearing, in Figs. 4 and 5, to be relatively pure in the separate gross structure components. Small corrections for the intrusion of adjacent groups have been applied for the 0.8 and 5.0-Mev groups, which corrections slightly accentuate structure evident in the uncorrected distributions but introduce none not already present.

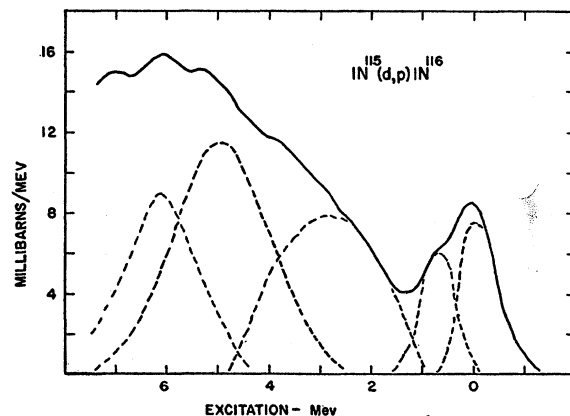


FIG. 5. Energy spectrum for  $\text{In}^{115}(d,p)\text{In}^{116}$  obtained by integrating Fig. 3 over angle; see Fig. 4 caption.

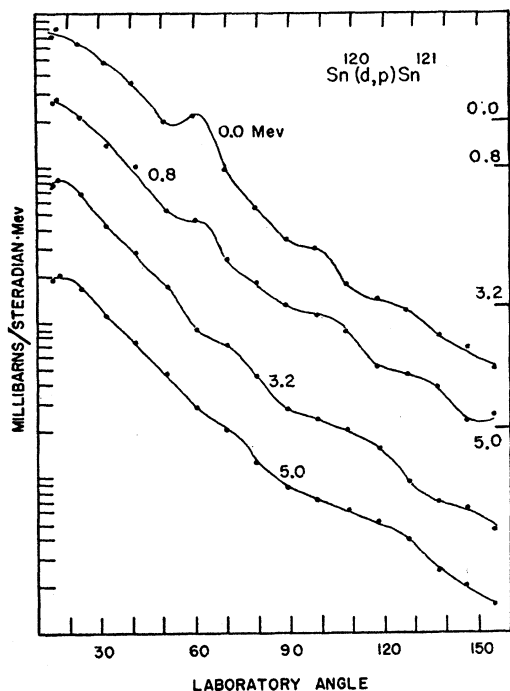


FIG. 6. Angular distributions of groups in  $\text{Sn}^{120}(d,p)\text{Sn}^{121}$ . Ordinates are taken from Fig. 2 at fixed excitations for each of which a single gross structure group predominates. Curves are displaced vertically for display; ordinate for 1.0 millibarn/steradian Mev is indicated at right for each of the curves. Points at the largest two angles are uncertain for the highest excitations.

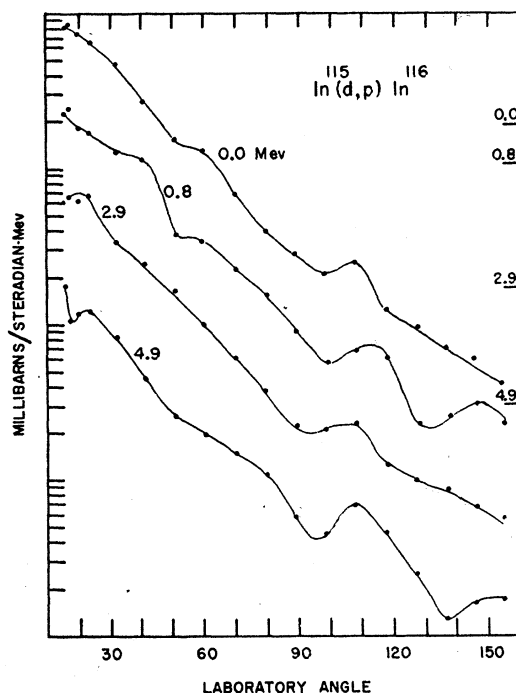


FIG. 7. Angular distributions of groups in  $\text{In}^{115}(d,p)\text{In}^{116}$ ; see Fig. 6 caption.

The overlap correction precludes a meaningful distribution for the 6.1-Mev group.

In summary, the experimental observations are: (1) a definite doublet at low excitation (group separation 0.8 Mev); (2) a marked minimum extending over the next 2 Mev; (3) structure at higher excitation which is weak but persistent and best represented by broad groups at 3 and 5 Mev; (4) angular distributions for various portions of the spectrum which are very similar but contain recurrent slight irregularities; and (5) a close similarity between the two reactions, in total cross section as well as in all the foregoing characteristics.

It is important to note that the weak definition of the gross structure (3) is not an instrumental effect. Over a similar excitation range Schiffer *et al.*<sup>8</sup> have found marked gross structure for Cr, Mn, and Fe with spacings of order 1–2 Mev. One expects similar spacings in the present experiment, since the first few single-particle spacings above the Fermi level show<sup>7</sup> no systematic trend with  $A$ , and indeed the intervals in our weak structure are of this same order which is also of the correct magnitude for single-neutron levels in a spherical nucleus (Table I and Appendix). Consideration of crystal resolution, straggling in absorbers and

channel width indicate an experimental resolution of order 1 Mev, which is probably a pessimistic estimate in view of the definition of elastically scattered particle groups. The spectra at low excitation give direct evidence that a group separation of 0.8 Mev can be recognized. We conclude that the difference in definition of the present structure and that in the lighter nuclei<sup>8</sup> reflects a difference in the nuclear situation rather than in the detection system.

## DISCUSSION

### Spectral Locations

It is possible that the 0.8-Mev group represents a single nuclear level. Both product nuclei have three true levels in the first 0.4 Mev of excitation<sup>8,9</sup> which certainly for  $\text{Sn}^{121}$  and probably for  $\text{In}^{116}$  are the single-neutron levels  $2d_{3/2}$ ,  $1h_{11/2}$ , and  $3s_{1/2}$ ; immediately above,  $\text{In}^{116}$  has six levels between 0.8 and 1.7 Mev.<sup>9</sup> These spacings are in agreement with the shell-dependent semiempirical level density formula<sup>10</sup> from which we may further deduce that in the present experiment we might well resolve nuclear levels below 1 Mev and certainly could not do so above 3 Mev. The level pattern in  $\text{Sn}^{121}$  above the low-lying isomeric group is not known, but an analogy exists in  $\text{Sn}^{119}$

<sup>8</sup> M. Goldhaber and R. D. Hill, *Revs. Modern Phys.* **24**, 179 (1952).

<sup>9</sup> Nuclear Data Cards (National Research Council, Washington, D. C.).

<sup>10</sup> T. D. Newton, *Can. J. Phys.* **34**, 804 (1956).

<sup>7</sup> Ross, Mark, and Lawson, *Phys. Rev.* **102**, 1613 (1956). Note erratum, *Phys. Rev.* **103**, 1906 (1956).

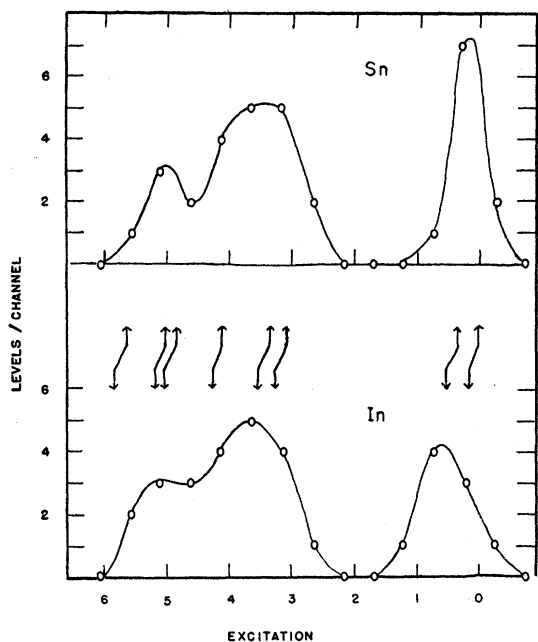


FIG. 8. Number of single-particle levels in the spheroidal well<sup>14</sup> occurring within one spectrometer channel, as a function of excitation (abscissa, Mev). Distortion parameters  $+0.08$  for  $\text{In}^{116}$ ,  $+0.04$  for  $\text{Sn}^{120}$ . Arrows show level positions in the undistorted Nilsson well, in order (right to left, increasing excitation):  $2d_{3/2}$ ,  $1h_{11/2}$ ;  $2f_{7/2}$ ,  $1h_{9/2}$ ;  $1i_{13/2}$ ;  $3p_{3/2}$ ,  $2f_{5/2}$ ;  $3p_{1/2}$ . Energy scale: see end of Appendix.

which has the same low-lying triplet and in addition a level at 0.9 Mev.<sup>9</sup> We conclude that the 0.8-Mev level found for both reactions could reflect a distinct nuclear level. It is not clear why this level appears strongly enough to be seen in our spectra whereas its neighbors do not, nor why this should be the case in both reactions. The level does not appear to match a single-particle excitation, and rotational collective levels are not to be expected so close to a stable spherical nuclear shape,<sup>11</sup> nor is it reasonable to expect the same rotational patterns for the two nuclei. It is possible that the level is a vibrational one, which might well be common to the two nuclei, although the 2-phonon vibrational energy in this region<sup>11,12</sup> is probably around twice the 0.8 Mev in question. Further, there is no clear reason to expect a vibrational state to be strongly excited in the  $(d,p)$  reaction.

Above 2 Mev true levels are certainly not resolved. There remain the questions of whether the pronounced minimum around 2 Mev and the broad groups around 3 and 5 Mev correspond to the pattern of single-neutron levels and, if so, why those groups are not more pronounced. These questions are related to the collective distortions of the nuclei concerned, a point of significant difference between this experiment and that with the

lighter nuclei<sup>3</sup> since that part of a given absolute distortion (as determined, e.g., from measured quadrupole moment) which must be assigned to the nuclear core increases markedly between the lighter nuclei and those of this experiment (see Fig. 3 of Ford and Hill<sup>13</sup>). The collective (core) distortion of  $\text{In}^{116}$  may be estimated from the measured quadrupole moment, the single-particle contribution, and the effective projection factor [reference 12, Eqs. (V.2), (V.10), and Table IX]. The distortion parameter (Nilsson<sup>14</sup>  $\delta$ ) is  $+0.08$ , which may be taken as a good estimate for  $\text{In}^{116}$  as well inasmuch as the same value is also found for  $\text{In}^{113}$ . As for Sn, although one expects small deformation because of the proton magic number, the deformation need not vanish absolutely since some polarizing effect of the unfilled neutron shell is to be expected. Indeed the existence of measurable isotope shifts among the Sn isotopes<sup>15</sup> shows that most of the intrinsic distortions must be finite. In particular, the measured shift for  $\text{Sn}^{122}$ - $\text{Sn}^{124}$  allows an estimate of the deformation parameter for  $\text{Sn}^{121}$  as about  $+0.04$ . The estimate may be roughly confirmed from first excited state systematics (see Figs. 4 and 5 of Ford<sup>16</sup>) which give a deformation parameter of  $+0.05 \pm 0.05$ . We conclude that the deformation parameters for  $\text{In}^{116}$  and  $\text{Sn}^{121}$  are of the order of  $+0.08$  and  $+0.04$ , respectively.

The effect of these deformations on single-particle levels<sup>14</sup> is to remove degeneracy to such an extent as apparently to disperse the spherical well pattern entirely. However, for these distortions the component levels diverge symmetrically about their origin in the spherical well, by amounts less than or comparable to the separations of the spherical well levels, the shifts generally occurring inside the resolution interval of this experiment. It follows that a single spectrometer channel will generally comprehend several of the spheroidal levels and so respond to the gross form of their distribution in energy, which itself reflects the original distribution of levels in the undistorted well. That this is the case, and particularly that the observed distribution will be similar for the two nuclei in spite of their differing distortions, is shown by Fig. 8. This represents a count of the spheroidal well levels<sup>14</sup> for  $\text{In}^{116}$  (67 neutrons, deformation  $+0.08$ , ground state  $=h_{11/2}$ ,  $1/2^-$  as dictated by this distortion) and  $\text{Sn}^{121}$  (71 neutrons, deformation  $+0.04$ , ground state  $=d_{3/2}$ ,  $1/2^+$ ). The ordinate is the number of spheroidal levels occurring within  $\pm 0.25$  Mev (roughly  $\pm 0.5$  channel) of the excitation abscissa. Positions of the original spherical well levels are indicated on the same

<sup>13</sup> K. W. Ford and R. D. Hill, *Annual Review of Nuclear Science* (Annual Reviews, Inc., Palo Alto, California, 1955), Vol. 5, p. 25. The regions of low distortion are readily identified in Fig. 3.

<sup>14</sup> S. G. Nilsson, Kgl. Danske Videnskab. Selskab, Mat.-fys. Medd. **29**, No. 16 (1955).

<sup>15</sup> P. Brix and H. Kopfermann, *Revs. Modern Phys.* **30**, 517 (1958).

<sup>16</sup> K. W. Ford, *Phys. Rev.* **90**, 29 (1953).

<sup>11</sup> K. Way *et al.*, *Annual Review of Nuclear Science* (Annual Reviews, Inc., Palo Alto, California, 1956), Vol. 6, p. 147.

<sup>12</sup> A. Bohr and B. R. Mottelson, Kgl. Danske Videnskab. Selskab, Mat.-fys. Medd. **27**, No. 16 (1953).

excitation scale,<sup>17</sup> i.e., relative to zero for the spheroidal well ground states.

It is clear that Fig. 8, although intended only to indicate qualitatively the reappearance of spherical well level positions when the spheroidal well is examined with poor resolution, reproduces the gross characteristics of the spectra observed in this experiment, *viz.*, the marked minimum around 2 Mev and broad maxima at 3 and 5 Mev. The minimum reflects the large single particle level spacing which is responsible for the magic number 82, and the two broad maxima correspond in position to the near coincidence of the pairs of single-neutron levels  $2f_{7/2}$ ,  $1h_{9/2}$  and  $3p_{3/2}$ ,  $2f_{5/2}$ . It is likely that the single-particle levels of the spheroidal well do contribute a structure to the spectra on a scale of separation of the same order as the energy resolution of this experiment. This would account for the observation in individual spectra of a number of "fluctuations" of greater than statistical magnitude (as attested by the statistical analysis performed on the ground-state intensities). Such fluctuations, being sensitive to the exact location of channel boundaries, would not be expected to reproduce in successive determinations and so would be eliminated from the "representative" spectra of Figs. 4 and 5.

It seems likely therefore that the structure reflecting true single-particle levels was not really resolvable in this experiment, but that the distribution of such levels, itself conditioned by the pattern of spherical well levels, may well be reflected in the weak gross structure which was observed. It remains to inquire whether the expected correlation in spectral positions exists between the gross groups and the two positions of near coincidence of spherical well levels. That this correlation exists is clear from Table I, in which the spherical well level positions (deduced from binding energy data; see Appendix) are compared with the gross structure.

Although not apparent in Fig. 8, the doublet from the low-excitation group is entirely consistent with the distribution of spheroidal well levels in that region.

### Angular Distributions

These are notable chiefly for their similarity. The relatively small peaks and inflections of Figs. 6 and 7 are most marked at the particular excitations plotted; distributions for arbitrary positions in the spectrum show less structure, and if integrated over successive 1-Mev portions of spectrum the distributions are almost perfectly superposable. The absence of the usually dramatic stripping minima cannot be attributed to the counter's acceptance angle, of order  $1^\circ$ , nor is it possible with any reasonable radius to extend the principal stripping peak over the full physical range.

<sup>17</sup> In obtaining Fig. 8 the energy scale of the Nilsson diagram has been adjusted to correspond to spherical well positions based on experimental mass differences; see end of Appendix.

TABLE I. Gross structure and single-neutron levels.<sup>a</sup>

Sn <sup>120</sup> ( $d, p$ )Sn <sup>121</sup>			In <sup>115</sup> ( $d, p$ )In <sup>116</sup>			Single neutron levels	
Exc. (Mev)	Width (Mev)	$\sigma$ (mb)	Exc. (Mev)	Width (Mev)	$\sigma$ (mb)		Exc. (Mev)
0.0	0.3	4.9	0.0	0.4	6.4	$\begin{cases} 2d_{3/2} \\ 1h_{11/2} \\ 3s_{1/2} \end{cases}$	$\begin{cases} 0.00 \\ 0.04 \\ 0.3 \pm 0.1 \end{cases}$
$0.8 \pm 0.1$	0.5	4.9	$0.8 \pm 0.1$	0.4	5.3	$\begin{cases} 2f_{7/2} \\ 1h_{9/2} \end{cases}$	$\begin{cases} 2.83 \pm 0.3 \\ 3.07 \pm 0.0 \end{cases}$
$3.2 \pm 0.2$	1.0	20.2	$2.9 \pm 0.5$	1.3	16.8	$\begin{cases} 2f_{5/2} \\ 3p_{3/2} \end{cases}$	$\begin{cases} 4.53 \pm 0.2 \end{cases}$
$5.0 \pm 0.1$	0.8	32.8	$4.9 \pm 0.4$	1.1	23.1		
			$6.1 \pm 0.1$	0.9	15.9		
$\leq 6.5$		70.8	$\leq 6.5$		63.8		
			$\leq 7.5$		78.6		

<sup>a</sup> Exc. = position of group peak (excitation of product nucleus) determined by averaging positions in all individual spectra. Width = half width at half maximum. Cross sections are integrated over angle and energy; totals include all contributions up to excitation limits specified. Single-particle levels are for spherical well and are deduced from binding-energy data (Appendix), the uncertainty in each referring to its separation from the preceding one.

Strong stripping minima are not to be expected within the interpretation of the preceding section, for in the distorted nucleus the single-particle  $l$  fails as an exact quantum number, and values of total nuclear spin are well mixed in the gross groups of Fig. 8. However, for the weak to intermediate coupling situation represented here,<sup>12,14</sup>  $l$  is an approximate constant of motion so we may anticipate for a gross structure group an angular distribution which, though largely smooth, may retain some traces of the maxima characteristic of the  $l$  value which predominates among the single particle levels it includes. In a similar fashion, in case of intermediate coupling, the energy spectrum is enhanced in the region of a single-particle excitation even when the latter fails as a constant of motion.

In fact even the  $l$  values are mixed to the extent of one to three values per gross structure group. Only the 0.8-Mev group is pure in  $l$  ( $h_{11/2}$  at the excitation chosen for the angular distribution). The 0-Mev group contains  $d_{3/2}$  and  $h_{11/2}$ , the 3-Mev group  $f_{7/2}$ ,  $h_{9/2}$ , and  $i_{13/2}$ , the 5-Mev group  $f_{5/2}$  and  $p_{3/2}$ . The  $i_{13/2}$  levels are widely dispersed; they are represented only weakly around 3 Mev and not at all around 5 Mev. Thus the parity is predominantly odd for all groups but pure only for those at 0.8 and 5 Mev. In case of mixed  $l$  values of the same parity, one expects the stripping structure to be lost at small angles but preserved at large ones for which the Bessel functions assume their asymptotic forms, in which case the  $l$  dependence degenerates to a parity dependence, leaving the large-angle peaks coincident for given parity.

On this basis the following qualitative features of the angular distributions are readily understood. (1) The strongest resemblances are for the same excitation in different reactions rather than for the same reaction at different excitations, suggesting as do the spectra that the operative mechanism is more sensitive to excitation than to the specific nucleus involved. The

angular structure is more marked for In than for Sn, presumably as a consequence of the use of an In target about half as thick as the Sn, resulting in better energy resolution. (2) The strongest resemblances among all groups occur at large angles. (3) The most pronounced structure at large angles occurs for the 0.8- and 5-Mev groups. (4) At small angles the structure is most pronounced for the 0.8-Mev group. (5) The largest number of peaks is found for the 0.8-Mev group. For these two groups the mean spacing of the observed peaks, interpreted as an interval in the stripping phase variable  $QR$ , is  $1.08\pi \pm 15\%$ . This should be of order  $\pi$  for a single  $l$  value or mixed  $l$  values of the same parity. The value quoted is based on a radius dictated by the condition that the observed number of peaks fall within the physical range, a rather restrictive condition. The radius so determined is  $7.9 \times 10^{-13}$  cm, in close agreement with the usual stripping radius  $(1.7 + 1.2A^{1/3}) \times 10^{-13}$  cm. With this radius, the stripping curve envelope declines with angle at a rate reasonably consistent with the observed gross form of distributions, as distinguished from the far faster variation over a single peak.

### Cross Sections

Significant stripping cross sections cannot be computed without the refinements of machine calculation, but their order of magnitude may be estimated by schematic models.<sup>18,19</sup> The rudimentary estimate for the range studied in these reactions is of order 50 mb, quite consistent with the observed 64 and 71 mb (Table I). Cross sections for a compound-nucleus process are of order 5 microbarns and 0.1 microbarn for Sn and In, respectively.

Both reactions have been examined previously at  $30^\circ$  in the laboratory (Harvey, reference 1 and private communication). In the In reaction the two determinations of the cross section of the 0 excitation group agree within 25% of the earlier determination, for which the quoted error is 40%. For the Sn reaction the isotopic abundance of the enriched target used by Harvey is not known, but an enrichment factor of 2 brings the intensities into agreement. For each reaction there is detailed agreement in the spectral shape substantiating the gross structure which has been discussed.

### ACKNOWLEDGMENTS

We acknowledge gratefully support by the John Simon Guggenheim Memorial Foundation (R.A.P.) and the Department of Scientific and Industrial Research (J.L.). Cordial thanks are extended (R.A.P.) to W. E. Burcham, G. W. Greenlees, and the Physics Department of the University of Birmingham for the hospitality of a productive and stimulating group.

<sup>18</sup> D. C. Peaslee, Phys. Rev. **74**, 1001 (1948).

<sup>19</sup> J. M. Blatt and V. F. Weisskopf, *Theoretical Nuclear Physics* (John Wiley & Sons, Inc., New York, 1952).

### APPENDIX. SINGLE-NEUTRON LEVELS IN SPHERICAL NUCLEI

Insofar as the observed spectra reflect the distribution of single-neutron levels, broad maxima are expected at energies corresponding to the positions in spherical nuclei ( $A \sim 120$ ) of three clusters of single-neutron levels, viz: Group I— $2d_{3/2}$ ,  $1h_{11/2}$ , and  $3s_{1/2}$ ; Group II— $2f_{7/2}$  and  $1h_{9/2}$ ; Group III— $3p_{3/2}$  and  $2f_{5/2}$ . The positions of levels in Group I are experimentally available from data on the isomeric states of the nuclei in question, but those of the higher clusters must be otherwise deduced. Direct calculation of the positions in a square well or oscillator potential is insufficiently accurate, as are the results of even more refined phenomenological potentials,<sup>7,14</sup> absolute level positions being most sensitive to the details of initial assumptions.

The sequence of single-neutron levels is known from the empirical filling order<sup>20,21</sup> for odd- $N$  even- $Z$  nuclei and the separation between any two successive levels may in principle be deduced from the difference between the last neutron separation energies of neighboring isotopes whose Fermi levels are, respectively, the two in question. For levels occupied only by neutron pairs in nuclear ground states, such as  $1h$ , the relevant separation energy is one half the difference between the separation energy for the neutron pair and the empirical pairing energy. Level positions so deduced refer to cores of assorted sizes ( $A$ ), and to produce a level scheme for a single nucleus it is necessary to adjust the raw spacings for change in  $A$ . The adjustment is straightforward in the case of a spherical square well of infinite depth. In this case the single-neutron levels are defined by unique values of the interior phase variable  $KR$  so that any single-neutron level position reflects a unique,  $A$ -independent value of  $EA^{\frac{2}{3}}$ ,  $E$  being the level position referred to the bottom of the well; any level position and all spacings are proportional to  $A^{-\frac{2}{3}}$ . This relation should remain a fair approximation for the finite square well, so long as the Fermi level remains much closer to the top of the well than to its bottom. However, other qualifications to this simple level adjustment require specific corrections.

Level positions are strongly affected by parameters of the diffuse nuclear surface and, of course, the spin-orbit interaction. However, it has been shown<sup>7</sup> that for a potential incorporating values of these parameters compatible with the empirical filling order, the elevation of any level in the realistic well above its position in the corresponding square well is a unique function of the diffuseness parameter, itself insensitive to  $A$ . This consideration and the foregoing lead to the defining relation

$$[V - e_a - B_a(A)]A^{\frac{2}{3}} = c_a, \quad (1)$$

and thence to the working formulas

$$B_a(A_2) = B_a(A_1) + c_a(A_1^{-\frac{2}{3}} - A_2^{-\frac{2}{3}}), \quad (2)$$

$$D_{ab}(A_2) = D_{ab}(A_1) + (c_a - c_b)(A_1^{-\frac{2}{3}} - A_2^{-\frac{2}{3}}), \quad (3)$$

$$c_a = c_b(A_1/A_2)^{\frac{2}{3}} + A_1^{\frac{2}{3}}[B_b(A_2) - B_a(A_1) + e_b - e_a]. \quad (4)$$

The subscripts  $a, b$  refer to particular levels and 1, 2 to different nuclei, isotopes in practice.  $B_a(A_1)$  represents the position of level  $a$  in the real nucleus of mass  $A_1$ , measured from the top of the well, and  $D_{ab}(A_1) = B_a(A_1) - B_b(A_1)$  is the separation between adjacent levels in a particular nucleus. The elevation of level  $a$  in the real well above its position in the corresponding square well is represented by  $e_a$ , independent of  $A$  as observed above, and  $V$  is the depth common to real and square wells, the same for all levels and nuclei. Equation (1) defines the quantity  $c_a$ , whose independence of  $A$  is a consequence of the foregoing arguments and is the basis of the method of level adjustment. The value of  $c_a$  could be determined from (1) on the basis of a single known occurrence of the level, given values<sup>7</sup> of  $V$  and  $e_a$ . However, in

<sup>20</sup> P. F. A. Klinkenberg, Revs. Modern Phys. **24**, 63 (1952).

<sup>21</sup> M. G. Mayer, in *Beta and Gamma Ray Spectroscopy*, edited by K. Siegbahn (North-Holland Publishing Company, Amsterdam, 1955), Chap. 16.



view of their considerable sensitivity to  $V$ , it is preferable to deduce the values of the  $c_a$  from binding data through (2)–(4), thereby utilizing only the constancy of  $V$  and not an *a priori* value. This procedure in effect determines  $V$  from the binding data, and the credibility of the values so obtained provides a plausibility check on the method of adjustment. Empirical evaluation of the  $c_a$  for each set of isotopes is the more important in that, through the  $B_a$  appearing in (1), they are expected to be somewhat sensitive to  $Z$ ; e.g., for  $Z=50$  the abnormally strong binding of levels suggests that the  $c_a$  will be abnormally small, as is found. When the appropriate  $c_a$  are known, Eqs. (2) and (3) provide for the translation to different  $A$  of a level and a spacing, respectively, and require no quantities other than those found empirically for the isotopes in question. For evaluating a particular  $c_a$ , Eq. (2) requires the level position to be known in two isotopes reasonably separated in  $A$ . When this information is lacking, Eq. (4) provides for the determination of  $c_a$  from a single occurrence of the level  $a$ , by comparison with another level on which more data are available. For this kind of determination it is necessary to use *a priori* values of the  $e_a$ , which have been taken from reference 7 and are (in Mev):  $2d_{3/2}$ , 2.55;  $1h_{11/2}$ , 5.31;  $2s_{1/2}$ , 1.72;  $2f_{7/2}$ , 1.70;  $1h_{9/2}$ , 5.86. The absolute well depth used in reference 7 is 40.8 Mev, but any value in the range  $45 \pm 10$  Mev seems reasonable.

The level positions  $B_a$  may be identified directly with neutron separation energies,  $S(A)=\text{mass of isotope } (A-1) + \text{mass of neutron} - \text{mass of isotope } (A)$ , only if the total binding energy of the core ( $A-1$ ) in isotope ( $A$ ) is the same as that of nucleus ( $A-1$ ). This is not the case, even ignoring interaction between last neutron and core, as shown by the slow but systematic decline of average binding energy per particle in the region  $A \geq 100$ . That this effect is important is immediately clear from the tabulated separation energies, which decline systematically with increasing  $A$  whereas the level bindings ( $B_a$ ) must, by the preceding arguments, increase. Thus instead of  $B_a(A)=S(A)$  when  $a$  is the Fermi level in  $A$ , we have

$$B_a(A) = S(A) + (A-1)[F(A-1) - F(A)], \quad (5)$$

where  $F(A)$  is the mean binding energy per nucleon in nucleus  $A$ . It is not appropriate to evaluate  $F$  in this correction term from mass data, since the observed value  $F(A)$  will depend upon  $B_a$  as well as the core. Instead, for the systematic behavior of the core it is appropriate to employ the semiempirical mass formula. So evaluated, the correction in (5) involves the surface, Coulomb, symmetry and pairing terms, for which the constants of Green<sup>22</sup> have been employed. The correction has the anticipated effect, yielding level bindings ( $B_a$ ) which increase with increasing  $A$  (compare Tables II, III). Since only differences among  $B_a$  values are used, the results are insensitive to any constant systematic error in the magnitude of the core variation correction, and only slightly sensitive to a systematic error varying with  $A$ .

The pairing term in the semiempirical mass formula, though appropriate to the representation of core behavior, is not adequate for use in the case of a Fermi level occupied by a neutron pair, for the semiempirical term is an average representation for all nuclides, from which the specific term required may be expected to deviate for particular ranges of nucleon numbers. An adequate power-law representation must be established for the range of  $A$  to be used. It is found from analysis of the Sn isotopes that  $PA^2 = \text{constant}$  is an adequate representation ( $P = \text{pairing energy}$ ), and the constant is evaluated independently for each set of isotopes used.

The last complication in the deduction of spherical well level positions from binding data is the sizable level shift arising from any appreciable nuclear distortion.<sup>14</sup> However, Fermi level positions initially deduced from undistorted nuclei and translated to the  $A$  of interest ( $\sim 120$ ) by the formalism outlined will provide the desired pattern of single-neutron levels for the spherical well

TABLE II. Neutron separation energies and excited configurations.<sup>a</sup>

A	Configuration	S,U	Source
Tin Isotopes			
115	$(s_{1/2})^1$	7.56±0.2	$b; r$
116	$(h_{11/2})^2$	9.37±0.28	$r$
117	$(h_{11/2})^2 (s_{1/2})^1$	7.17±0.37	$i, b; m$
117	$(h_{11/2})^2 (d_{3/2})^1$	0.161	$i$
117	$(h_{11/2})^3$	0.320	$i$
118	$(h_{11/2})^4$	9.10±0.2	$r$
119	$(h_{11/2})^4 (s_{1/2})^1$	6.54±0.12	$i, b; r$
119	$(h_{11/2})^4 (d_{3/2})^1$	0.024	$i$
119	$(h_{11/2})^6$	0.089	$i$
120	$(h_{11/2})^6$	8.95±0.34	$m$
121	$(h_{11/2})^6 (d_{3/2})^1$	6.14±0.07	$i, b; r$
121	$(h_{11/2})^7$	0.037	$i$
122	$(h_{11/2})^8$	8.73±0.10	$m$
123	$(h_{11/2})^8 (d_{3/2})^1$	5.96±0.48	$i, b; m+r$
123	$(h_{11/2})^9$	0.00	$i$
124a	$(h_{11/2})^{10}$	8.50±0.15	$r$
125	$(h_{11/2})^{11}$	5.74±0.07	$i, b; r$
125	$(h_{11/2})^{10} (d_{3/2})^1$	0.036	$i$
Xenon isotopes			
127	$(h_{11/2})^8 (s_{1/2})^1$	~7.245	$i, b; r$
127	$(h_{11/2})^8 (d_{3/2})^1$	0.125	$s$
127	$(h_{11/2})^9$	0.300	$i$
129	$(h_{11/2})^{10} (s_{1/2})^1$	6.91±0.33	$i, b; m$
129	$(h_{11/2})^{10} (d_{3/2})^1$	0.039	$i$
129	$(h_{11/2})^{11}$	0.235	$i$
131	$(h_{11/2})^{12} (d_{3/2})^1$	6.60±0.05	$i, b; j$
131	$(h_{11/2})^{12} (s_{1/2})^1$	0.080	$i$
132a		8.92±0.07	$j$
133		6.74±0.08	$j$
134a		8.24±0.07	$j$
135	$(h_{11/2})^{12} (d_{3/2})^3 (s_{1/2})^2$	6.55±0.10	$i, b; j$
136a	$(h_{11/2})^{12} (d_{3/2})^4 (s_{1/2})^2$	7.91±0.09	$j$
137	$(2f_{7/2})^1$	4.47±1.0	$b; j$
Barium isotopes			
133	$(s_{1/2})^1$	7.68±0.19	$i, b; j+r$
133	$(d_{3/2})^1$	0.012	$i$
134a		9.26±0.14	$r$
135	$(d_{3/2})^3$	6.85±0.12	$i, b; j$
136		9.18±0.12	$j$
137	$(d_{3/2})^3 (s_{1/2})^2$	6.99±0.09	$i, b; j$
137	$(d_{3/2})^4 (s_{1/2})^1$	0.281	$s$
138a	$(d_{3/2})^4 (s_{1/2})^2$	8.67±0.09	$j$
139	$(2f_{7/2})^1$	4.717±0.01	$b; r$
140	$(i h_{9/2})^2$	6.43±0.15	$j$

<sup>a</sup>  $S, U$  designates neutron separation energy for ground-state configuration and excitation for higher configurations (following) in same nucleus. "Sources" of data ( $r, m, j$ ) and configurations ( $i, b, s$ ) are:  $r$ =nuclear reactions [R. W. King, *Revs. Modern Phys.* **26**, 327 (1954); L. J. Lidofsky, *Revs. Modern Phys.* **29**, 773 (1957); D. M. Van Patter and W. Whaling, *Revs. Modern Phys.* **29**, 757 (1957) and reference 6],  $m$ =mass spectroscopic data [H. E. Duckworth *et al.*, *Revs. Modern Phys.* **26**, 463 (1954); **29**, 767 (1957)],  $j$ =a self-consistent set of mass spectroscopic determinations [W. H. Johnson, Jr., and A. O. Nier, *Phys. Rev.* **105**, 1014 (1957)],  $i$ =nuclear isomer assignment (reference 8),  $b$ =beta decay assignment (reference 21),  $s$ =assignment from spin value (reference 9). The two-neutron separation energy for any nucleus is the sum of the single-neutron separation energies listed for it and its predecessor. However, for nuclei marked  $a$  the uncertainty in the two-neutron separation energy is substantially less than the combination of uncertainties in the two contributing values.

near  $A=120$ . Nuclei especially suitable as sources of data are those for which each nucleon number is nearly magic,<sup>13</sup> for which  $Z$  is even (to avoid complications of cross-pairing energy) and for which reliable mass data are available.

The starting data for the present calculations are presented in Table II, involving tin isotopes of 65 to 75 neutrons, xenon isotopes of 73 to 83 neutrons, and barium isotopes of 77 to 84 neutrons. It appears that a slight proton excess (over 50) and neutron deficiency (below 82) act together to maintain low distortion over these isotopic ranges. From the separation energies and configuration excitations of Table II the positions of the single-neutron levels in the various nuclei are obtained by cor-

<sup>22</sup> A. E. S. Green, *Phys. Rev.* **95**, 1006 (1954).

TABLE III. Corrected level positions in tin isotopes.<sup>a</sup>

A	$B_d$ (Mev)	$B_s$ (Mev)	$B_h$ (Mev)
116		10.478	
117	10.459	10.620	10.300
119	10.501	10.498	10.409
121	10.572		10.535
123	10.883		10.833
125	10.992		10.834

<sup>a</sup> Body of table gives ( $B$ , Mev) position below top of well of level in Sn isotope of mass indicated (including the "single" neutron), obtained from the neutron separation energies of Table II corrected for variation in the binding energy of the core. Levels are designated by subscripts  $d$  ( $2d_{3/2}$ ),  $h$  ( $1h_{11/2}$ ), and  $s$  ( $3s_{1/2}$ ). Nonsignificant figures are carried to show values of the core correction; for applicable uncertainties see Table II.

rection for core variation, through equation (5). The results are given in Table III for the tin isotopes; in the cases of xenon and barium the trustworthy level deductions are less regular and will be cited in the appropriate discussions.

### Tin Isotopes

The level positions shown in Table III are free of pairing energy complications and provide a direct check on the proposed adjustment formula (1). The  $d$  and  $h$  level data fit straight lines when plotted against  $A^{-3}$ , with positive slopes  $c_d=320$  and  $c_h=330$ , the main deviations being 0.06 and 0.05 Mev, respectively. Clearly the three  $s_{1/2}$  values do not form a straight line, but the first two define a slope  $c_s=280$ . The relative magnitudes of these slopes confirm the *a priori* expectation; the  $d_{3/2}$  level being more strongly bound than  $h_{11/2}$ , we expect  $c_d < c_h$ , and similarly the  $s_{1/2}$  level being the lowest (for the first two isotopes in Table III) we expect  $c_s$  to be the smallest of the three slopes. In effect this verifies an expected correlation of slope with intercept in the  $B$ - $A$  plots. Values of  $V$  implied by the observed slopes and intercepts are 26.4 Mev (from  $d_{3/2}$ ) and 29.5 Mev (from  $h_{11/2}$ ); their consistency is an additional check of the method, and their low absolute magnitude may reasonably be attributed to the anomalous core situation at  $Z=50$ .

In addition to the data in Table III we have a good value of the two-neutron separation energy in each of ten isotopes, each representing a neutron pair in  $h_{11/2}$ . The five values for odd  $A$  may be used to determine the *de facto* pairing energy in this region, by comparison with the single-neutron separation energies from the singly occupied  $h_{11/2}$  configuration in the same nuclei. The five pairing energies so obtained have been tested for constancy of the product  $PA^n$  and the following deviations from constancy found:  $n=0$ , 2.0%;  $n=\frac{1}{2}$ , 1.3%;  $n=\frac{3}{4}$ , 1.6%;  $n=1$ , 1.7%. We conclude that  $PA^{\frac{1}{2}}=\text{constant}$  is the best representation. The value of this constant ( $30.7\pm 0.4$ ) is roughly three times the average pairing energy term in the semiempirical mass formula, which is quite reasonable in view of the fact that the nucleus is proton-magic and that the level involved is the highly asymmetric  $h$  level. It is apparent from the filling order that pairing in this level is sufficiently strong to depress it below  $s_{1/2}$  and  $d_{3/2}$  for even neutron numbers.

The two-neutron separation energies for the five even- $A$  isotopes may now be used, with the empirical pairing energy just deduced from the odd- $A$  isotopes, to give an additional independent check of the adjustment formula. The  $h_{11/2}$  level positions ( $B_h$ ) so deduced fit a straight line against  $A^{-3}$  with mean deviation 0.03 Mev, the slope checking the previous determination ( $c_h$ ) within 15% and the value of  $V$  within 7%.

The isomeric state data of Table II give the relative positions of the levels in Group I for  $\text{Sn}^{121}$  without further adjustment, and locate  $1h_{11/2}$  at 0.037 Mev above the ground state ( $2d_{3/2}$ ). Systematics of the isomeric states in this region<sup>8</sup> allow a good estimate of the position of  $3s_{1/2}$  in the same nucleus, at about

0.3-Mev excitation. Level shifts resulting from translation to  $A=116$  (for the indium case) are all less than 0.05 Mev. Clearly the levels within Group I could not be resolved in the experiment reported.

### Xenon Isotopes

The following usable level information is obtained by core-correction of data of Table II (subscripts refer to levels;  $f=2f_{7/2}$ , others as before):

$$A=127, \quad B_s=10.835 \text{ Mev}, \quad B_s-B_d=0.125 \text{ Mev}, \\ B_s-B_h=0.300 \text{ Mev};$$

$$A=129, \quad B_s=10.964 \text{ Mev}, \quad B_s-B_d=0.039 \text{ Mev}, \\ B_s-B_h=0.235 \text{ Mev};$$

$$A=131, \quad B_d=11.086 \text{ Mev}, \quad B_d-B_s=0.080 \text{ Mev};$$

$$A=135, \quad 2B_d+2B_s+2P=50.405 \text{ Mev};$$

$$A=136, \quad B_d+P=13.369 \text{ Mev};$$

$$A=137, \quad B_f=10.092\pm 1.0 \text{ Mev}.$$

The fourth and fifth lines, together with one absolute location and one separation chosen from the first three lines provide three simultaneous equations from which may be determined the  $c_a$  and  $c_b$  of the two levels concerned, and the constant  $PA^{\frac{1}{2}}$ . Equation (4) then allows  $c_f$  to be evaluated by comparison with either of the lower levels. These having been determined, the position of either of the levels may be translated to  $A=137$ , the separation between it and  $2f_{7/2}$  determined at  $A=137$ , and translated finally to  $A=120$ , by Eqs. (2) and (3). The first three lines provide five independent sets of starting data, and the consistency of the results derived constitutes an additional check of the method.

The extrapolation constants obtained are in the sequence  $c_h < c_d < c_s$ , an order opposite to that of the corresponding  $B$  values; i.e., the expected correlation of slopes and intercepts is again observed. All three values are much smaller than their counterparts in the Sn isotopes, as is the constant  $PA^{\frac{1}{2}}$ , confirming the consequences of qualitative arguments in the Sn discussion. Mean deviations among the values for the constants  $c_s$ ,  $c_d$ ,  $c_h$ ,  $c_f$ ,  $PA^{\frac{1}{2}}$ , and  $V$  based on different choices of starting data are of order 20% in all cases which, though large, represent consistency within the combined uncertainties in the starting data. Numerical values obtained are  $PA^{\frac{1}{2}}=13\pm 2$  Mev and  $V=51\pm 10$  Mev, both of which are physically reasonable and the former now only 30% higher than the pairing term in the semiempirical mass formula.

Fortunately the value for the position of the  $2f_{7/2}$  level relative to  $2d_{3/2}$  is substantially less sensitive to uncertainties in the starting data than are the working constants just discussed. Deviations in this quantity resulting from alternative choices of starting data are of order 8% and the weighted mean value is 2.80 Mev. The limits  $+0.25$  Mev,  $-0.15$  Mev include the full variation of independent determinations, but do not include the systematic uncertainty ( $\pm 1.0$  Mev) associated with the  $\text{Xe}^{137}$  separation energy.

### Barium Isotopes

The following level information (from Table II, corrected) is used ( $h=1h_{9/2}$ ;  $d, s, f$  as before):

$$A=133, \quad B_s-B_d=0.012 \text{ Mev}, \quad B_s=11.558 \text{ Mev};$$

$$A=137, \quad B_s-B_d=0.281 \text{ Mev};$$

$$A=135, \quad 2B_d+P=24.534 \text{ Mev};$$

$$A=137, \quad 2B_s+P=25.399 \text{ Mev};$$

$$A=139, \quad B_f=9.801 \text{ Mev};$$

$$B=140, \quad 2B_h+P=21.505 \text{ Mev}.$$

These are sufficient for a single determination of the positions of  $2f_{7/2}$  and  $1h_{9/2}$  in the spherical well at  $A=120$ . The first four lines provide three equations relating  $c_s$ ,  $c_d$ , and  $PA^{\frac{1}{2}}$ , and the last two lines give one good occurrence of each of the two Group II levels. The extrapolation constants  $c_f$  and  $c_h$  may thereby be determined

(Eq. 4) by reference to  $c_s$ . Finally the separations  $B_s(139) - B_f(139)$  and  $B_s(140) - B_f(140)$  may be determined and translated to  $A=120$ .

The constant found for  $PA^{\frac{1}{2}}$  differs by only 0.3% from that found from the Xe data, and the value of  $V$  ( $36.7 \pm 6.5$  Mev) is again physically reasonable though very sensitive to the starting uncertainties. Since there are two independent data at  $A=133$ , the computations may be carried through with reference either to the  $d_{3/2}$  or  $s_{1/2}$  level, the consistency again providing a measure of the reliability of the method. The  $2f_{7/2}$  level is found to lie above the  $2d_{3/2}$  ground state by  $2.86 \pm 0.33$  Mev at  $A=120$ , in agreement with the Xe determination, and  $1h_{9/2}$  is found above  $2f_{7/2}$  by  $0.235 \pm 0.003$  Mev. The anticipated crossing of those two levels between  $A=140$  and  $A=120$  is reproduced by the level adjustment method.

### Group III Levels

Since the levels of Group III are filled in the strong-coupling region, mass data cannot be applied as in the foregoing to locate Group III in the spherical well. However, the position of  $2f_{5/2}$ , and hence of Group III, may be fixed relative to its spin-orbit partner  $2f_{7/2}$ , already located, by comparison with the spin-orbit separation  $1h_{9/2} - 1h_{11/2}$ .

The separation of a spin-orbit doublet is proportional to the term  $(2l+1)$  and to the expectation value of  $r^{-1}(dV/dr)$ , the remaining proportionality factor being an absolute constant. The ratio of the first factor, for the splits in  $f$  and  $h$  levels, is of course  $7/11$ ; it is necessary to consider the ratio of the expectation value in the two cases, which may be identified as  $f(n, l)$ . It is reasonable to suppose that the ratio  $f(2f)/f(1h)$  is close to unity, since this is implied both by oscillator and square well potentials, which bracket the order of shell-model levels. It is exactly the case that the  $f$  ratio is unity for an oscillator potential, and for a square well it is approximately the case for single-particle states of the same parity insofar as the value of the interior phase variable  $(KR)$  is large compared to  $l$  so that the spherical Bessel function approximates its asymptotic form. In the present case (the  $2f$  and  $1h$  levels at  $A=120$ ) the phase variable is not less than 11 and  $l$  not greater than 5. That the approximation is sufficient is

indicated numerically by the relative spin-orbit splits resulting from Nilsson's spherical well calculation,<sup>14</sup> which are exactly in the ratio of  $(2l+1)$ . The proposition that  $f(n_1 l_1)/f(n_2 l_2)$  is unity may be tested against experimental data in the specific case that  $n_1+l_1=5$  and  $n_2+l_2=6$  (as for  $2f$  and  $1h$ ) by reference to separations<sup>23</sup> of the  $2g$  and  $3d$  doublets in the spherical nuclei  $Pb^{209}$  and  $Bi^{210}$ , for both of which the ratio is 0.87.

We may conclude that the ratio  $f(2f)/f(1h)$  lies between 0.87 and 1.00, from which, and the positions deduced in the foregoing, it follows that at  $A=120$  the level  $2f_{5/2}$  lies above  $2f_{7/2}$  by  $1.70 \pm 0.12$  Mev and so above the ground state ( $2d_{3/2}$ ) by  $4.53 \pm 0.45$  Mev. The ratio of the two spin-orbit splittings is not sensitive to nuclear radius since the absolute parameters of the well affect the splitting only through a constant factor  $V/R^2$ , for both oscillator and square well potentials.

A wholly independent though rough check of the separations found for the  $2f$  and  $1h$  doublets may be obtained by adjustment of the corresponding separations in the nuclei around  $A=208$  in proportion to the absolute factor just mentioned. To adjust from  $A=208$  to  $A=120$  in proportion to  $V/R^2$  for constant well depth, multiplication by  $(208/120)^{\frac{1}{2}}$  is required. For the heavy nuclei<sup>23</sup> we have  $f(2g)=f(n+l=6)=(2.05 \pm 0.15)/9$  and  $f(3d)=f(n+l=5)=(0.99 \pm 0.13)/5$ . Multiplying by the size factor we obtain, for  $A=120$ ,  $f(6)=f(1h)=0.33 \pm 0.02$  and  $f(5)=f(2f)=0.29 \pm 0.04$ , and hence the spacings  $3.6 \pm 0.3$  Mev ( $1h$ ) and  $2.0 \pm 0.3$  Mev ( $2f$ ). These are in reasonable agreement with the values already deduced, *viz.*,  $3.0 \pm 0.3$  Mev and  $1.7 \pm 0.1$  Mev.

The single-neutron level positions are summarized in Table I. To obtain Fig. 8 it was necessary to determine the energy scale of the Nilsson level diagram,<sup>14</sup> which was done by reference to the separation of the spin-orbit doublet  $1h_{9/2} - 1h_{11/2}$ . On this basis the energy unit of the Nilsson diagram is 5.5 Mev, or 0.66 times the magnitude estimate in the caption to Fig. 5 of reference 14. With this scale factor the level positions deduced in this Appendix for all other levels agree well with the spacings of Nilsson's spherical case, with the exception of  $2d_{3/2}$  which is misplaced in the Nilsson diagram as shown by the isomeric-state data.<sup>8</sup>

<sup>23</sup> B. B. Kinsey, *Handbuch der Physik*, edited by S. Flugge (Springer-Verlag, Berlin, 1957), Vol. XL, Pt. I, p. 362.